BMC Cancer

RESEARCH Open Access

Prediction of pathological response to neoadjuvant immunochemotherapy with baseline and post-treatment ^{18}F-FDG PET imaging biomarkers in patients with locally advanced gastric cancer

Mimi Xu[1†], Yafei Zhang[1†], Kui Zhao[1], Haiping Jiang[2], Guangfa Wang[1], Yan Wu[1], Yu Wang[3], Nian Liu[1*] and Xinhui Su[1*]

Abstract

Background Neoadjuvant immunochemotherapy (NICT) has shown promising therapeutic benefits in patients with locally advanced gastric cancer (LAGC). Our study aimed to predict the pathological response to NICT in LAGC before surgery by correlating the metabolic parameters of baseline and post-treatment ^{18}F-fluorodeoxyglucose (^{18}F-FDG) positron emission tomography/computed tomography (PET/CT) of the primary lesion with the pathological response following radical surgery.

Methods Thirty-six LAGC patients who received three cycles of NICT (combination of sintilimab and CapeOx), followed by radical surgery, were included in this study. Both baseline ^{18}F-FDG PET/CT (bPET) and post-treatment ^{18}F-FDG PET/CT (pPET) were conducted, the metabolic parameters derived from the PET/CT scans, including the maximum standardized uptake value (SUV_{max}), metabolic tumor volume (MTV), and total lesion glycolysis (TLG) on bPET and pPET ($bSUV_{max}$ and $pSUV_{max}$, bMTV and pMTV, bTLG and pTLG), as well as their reductions post-treatment (ΔSUV_{max}, ΔMTV, and ΔTLG), were assessed for their correlation with treatment efficacy and tumor regression grade (TRG) following NICT.

Results Out of the 36 patients, 13 patients had a good response (GR), which included 5 cases with TRG 0 and 8 cases with TRG 1. Conversely, 23 patients exhibited a poor response (PR), with 20 patients having TRG 2 and 3 patients having TRG 3. Univariate analysis revealed that pMTV and pTLG in the GR group were significantly lower compared to the PR group (all $p < 0.05$). The identified cutoff values of pMTV and pTLG were 1.68 cm^3 (area under the cure (AUC) = 0.683) and 4.71 cm^3 (AUC = 0.683) for the GR and PR groups, respectively. On receiver operating characteristic (ROC) curve analyses, these values corresponded to sensitivity, specificity, and accuracy of 68.8%, 80.0%, and 73.1%,

†Mimi Xu and Yafei Zhang contributed equally to this work.

*Correspondence:
Nian Liu
liuniancheer@gmail.com
Xinhui Su
suxinhui@zju.edu.cn

Full list of author information is available at the end of the article

respectively, with no statistically significant differences between them after the DeLong test and McNemar test (all $p > 0.05$). Furthermore, $bSUV_{max}$, bMTV, bTLG, ΔSUV_{max}, ΔMTV, and ΔTLG in the TRG 0 group were significantly higher than those in the TRG 1 group (all $p < 0.05$). Upon performing ROC curve analyses for the TRG 0 group, the thresholds for $bSUV_{max}$, bMTV, bTLG, ΔSUV_{max}, ΔMTV, and ΔTLG were determined to be 7.8 (AUC = 0.916), 36.76 (AUC = 0.768), 105.55 (AUC = 0.819), 4.82 (AUC = 0.923), 22.64 (AUC = 0.807), and 104.7 (AUC = 0.845), with no statistically significant differences between them after the DeLong test (all $p > 0.05$). These thresholds demonstrated high sensitivity (80% for bMTV and 100% for others), specificity (83.9%, 71.0%, 67.7%, 83.9%, 61.3%, and 71.0%), and accuracy (86.1%, 66.7%, 72.2%, 86.1%, 66.7%, and 75.0%) in predicting TRG 0 after NICT, with no statistically significant differences between them after the McNemar test (all $p > 0.05$).

Conclusions Imaging biomarkers from the combination of baseline and post-treatment ^{18}F-FDG PET/CT showed potential in predicting pathological response to NICT in LAGC patients before surgery.

Keywords Gastric cancer, PET/CT, Immunochemotherapy, Metabolic parameters

Introduction

Gastric cancer (GC) is a prevalent malignant neoplasm, ranking as the third leading cause of cancer-related mortality worldwide [1, 2]. GC patients are often diagnosed with locally advanced gastric cancer (LAGC) at their initial visit due to its atypical symptoms [1]. Despite moderate improvements in survival rates attributed to the combination of neoadjuvant therapy (NAT) and radical surgery, the prognosis of LAGC remains a significant challenge in oncological surgery [3]. Achieving a pathological complete response (pCR) following NAT is a crucial factor in improving survival rates for GC patients after surgery [4, 5]. Neoadjuvant immunochemotherapy (NICT) is an emerging NAT strategy for advanced GC, showing promise in promoting tumor regression [6, 7]. This approach integrates chemotherapy with immune checkpoint inhibitors (ICIs), specifically targeting programmed cell death protein 1 (PD-1) and programmed death-ligand 1 (PD-L1). It has shown significant efficacy in the management of advanced gastrointestinal malignancies and holds promise for promoting tumor regression through the combined action of chemotherapy and ICIs. NAT is widely acknowledged as a standard first-line therapeutic approach for LAGC, and anti-PD-1/PD-L1 therapies have shown robust and durable responses in advanced GC, with response rates of 10–26% in clinical trials [6]. Despite the promising outcomes, NICT-treated GC patients exhibit varied and limited response rates due to tumor heterogeneity and potential immunotoxicity [6]. Precisely predicting which NICT-treated patients will benefit before surgical intervention is crucial, as GC patients achieving a pCR to NAT prior to surgery have significantly better outcomes than those untreated [4, 5].

The pathological tumor regression grade (TRG) is currently considered the gold standard for evaluating the efficacy of NAT [8]. However, the delay in pathological evaluation makes it difficult to devise the best individualized treatment plans preoperatively. Conventional imaging modalities like computed tomography (CT) and magnetic resonance imaging (MRI) are typically used to assess responses to NAT. Yet, they struggle to accurately differentiate viable tumors from necrotic or fibrotic tissue and cannot reliably distinguish pseudo-progression or hyper-progressive disease. These limitations arise because CT and MRI assess responses based solely on structural changes in the tumor [9–12]. ^{18}F-fluorodeoxyglucose (^{18}F-FDG) positron emission tomography/computed tomography (PET/CT) is increasingly used to early assess responses to NAT by measuring changes in metabolic parameters, such as maximum standardized uptake value (SUV_{max}), metabolic tumor volume (MTV), total lesion glycolysis (TLG) [13–15]. However, their applicability and reliability in GC remain subjects of debate [16–18]. Furthermore, the impact of immunotherapy on primary tumors can complicate the interpretation of ^{18}F-FDG PET/CT scans, thus making the application of ^{18}F-FDG PET/CT in predicting the efficacy of immunotherapy even more challenging [6, 9–11, 19]. Atypical response patterns such as pseudoprogression, hyperprogression, dissociated response, and delayed response, which can result from immunotherapy, highlight the potential of ^{18}F-FDG PET/CT to surpass traditional imaging methods in predicting treatment responses [19]. However, these patterns also present significant challenges in the accurate interpretation of ^{18}F-PET/CT scans [20]. This complexity may stem from the intricate nature of the tumor microenvironment, characterized by the infiltration of immune and inflammatory cells, edema, and necrosis within the tumor following immunotherapy [6, 10]. These factors, in turn, influence the lesion's morphology and metabolic changes, leading to increased ^{18}F-FDG PET/CT metabolic activity and tumor volume enlargement, and ultimately resulting in the phenomena of pseudoprogression and hyperprogression observed on ^{18}F-FDG PET/CT scans. On the contrary, the immune activation process exhibits considerable variability among individuals, with some patients potentially displaying a delayed onset of immunotherapy efficacy and

a slow reduction in tumor size, which is manifested as a delayed response [19].

Currently, the assessment value of ^{18}F-FDG PET/CT in NICT has been focused on non-small cell lung cancer and melanoma, with some studies also evaluating the role of ^{18}F-FDG PET/CT in predicting the pathological response to NICT for resectable esophageal squamous cell carcinoma (ESCC) [7, 21, 22]. To our knowledge, it is important to note that there is a relative scarcity of research specifically addressing GC in this regard. The present results fully demonstrate the potential of ^{18}F-FDG PET/CT for evaluating immunotherapy and highlight the challenges due to tumor heterogeneity and the complex immune restoration process induced by immunotherapy [9, 10]. Nonetheless, there are currently no accepted indicators to assess pathological responses to NICT using ^{18}F-FDG PET/CT, indicating a need for further investigation.

Recognizing the critical importance of identifying GC patients who are most likely to benefit from NICT and achieve a pCR prior to surgery, our study was designed to identify imaging biomarkers of bPET and pPET in LAGC patients to predict pathological response to NICT before surgery early, and non-invasively, aiming to enhance the precision of surgical planning and therapeutic decision-making. We conducted a retrospective analysis to establish the correlation between metabolic parameters derived from bPET and pPET scans and the pathological responses to the NICT protocol, namely, sintilimab plus CapeOx (capecitabine and oxaliplatin), in LAGC patients who underwent radical surgery.

Materials and methods

Patients

This is a single-center retrospective study, approved by Clinical Research Ethics Committee of the First Affiliated Hospital of Zhejiang University School of Medicine (No.20230569), and the requirement for written informed consent was waived. LAGC patients who received three cycles of NICT (Sintilimab in combination with CapeOx) and underwent bPET and pPET from August 2019 to October 2020 at our hospital and were retrospectively analyzed. The inclusion criteria were as follows: (1) confirmed by gastroscopic biopsy to have gastric adenocarcinoma without previous chemotherapy, radiotherapy, targeted therapy, and immunotherapy; (2) had a clinical stage of cT_{3-4}, N_x, and M_0 according to the eighth edition of the American Joint Committee on Cancer (AJCC) Gastric Cancer Staging [23], as assessed by contrast-enhanced CT of the abdomen and pelvis; and (3) had radical surgical resection after NICT. The exclusion criteria were as follows: (1) secondary malignancy; (2) different or unknown therapeutic regimen; (3) significant physiological uptake in the gastric wall; (4) unfilled gastric cavity due to severe pyloric obstruction; (5) patients with signet-ring cell carcinoma. Finally, 36 patients were enrolled according to the inclusion criteria (Fig. 1).

Treatment regimen

The patients received three cycles of NICT before surgery, tailored to their conditions. The NICT consisted of sintilimab (3 mg/kg for cases < 60 kg and 200 mg for those ≥ 60 kg) intravenously on day 1, oxaliplatin (130 mg/m^2) intravenously on day 1 and capecitabine (1000

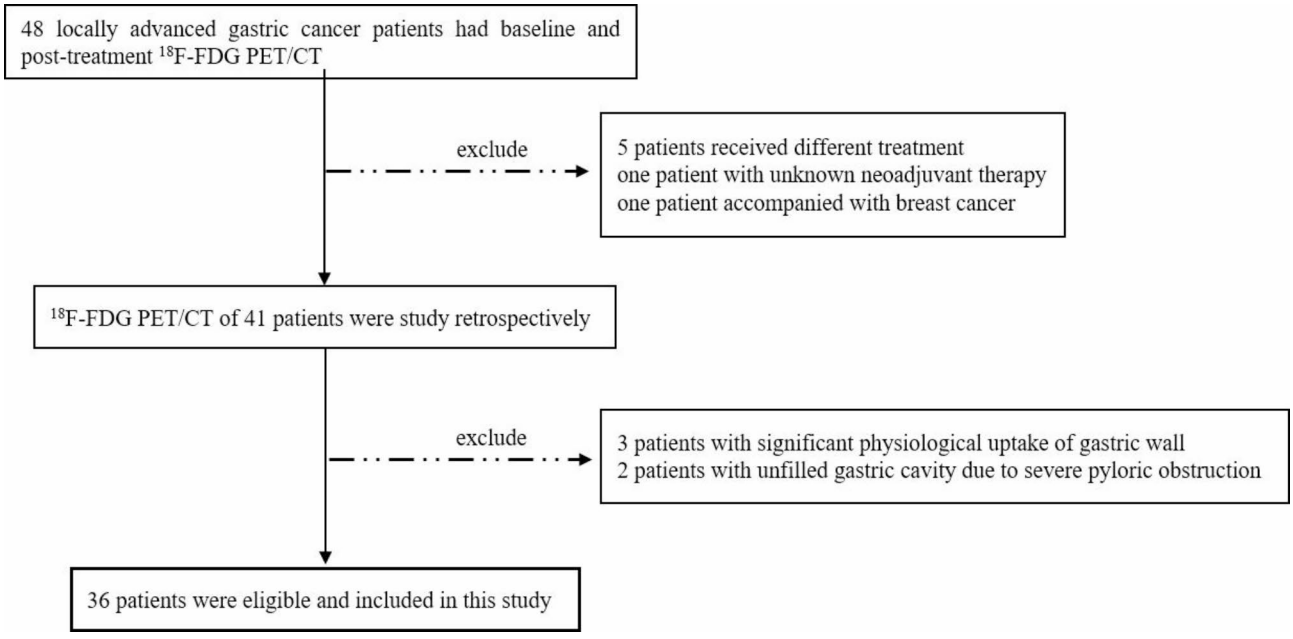

Fig. 1 Flow chart of patients selection

mg/m^2 two times per day) orally at days 1–14 for three cycles. The surgical procedure was gastrectomy with D_2 lymphadenectomy (lymph node dissection), which was performed 2 weeks after the third cycle.

PET/CT acquistion

The patients underwent PET/CT imaging using an integrated PET/CT scanner (Biograph mCT with 64-slice, Siemens Healthineers, Germany) with ^{18}F-FDG as the tracer (prepared by our PET center, synthesizer module with FDG4 Explora, Siemens Healthineers, Germany). Each patient was fasted for at least 6 h and had normal blood glucose levels (4.5–6.5 mmol/L) before the injection of ^{18}F-FDG (3.70–5.55 MBq/kg). They drank as much water (500 – 800 ml warm water) as possible to fill the stomach cavity. ^{18}F-FDG PET/CT scan was performed 60 min after ^{18}F-FDG injection from the top skull to the mid-thigh with three minutes per frame 3D acquisition. Low-dose CT (120 mAs, 120 kV, 512 × 512 matrix) was acquired to conduct attenuation correction and provide anatomical information. PET was reconstructed by using the Ordered Subset Expectation Maximization (OSEM) iterative method.

^{18}F-FDG PET/CT image analysis

All ^{18}F-FDG PET/CT imaging was interpreted by two experienced nuclear physicians at eSoft Workstation. The SUV_{max} of the gastric target lesion was automatically measured, and the volume of interest (VOI) was delineated by an automated contouring program. Similarly, the MTV and TLG of the gastric target lesions were also measured with a threshold $SUV_{max} > 2.5$. Metabolic parameters on bPET were $bSUV_{max}$, bMTV, bTLG, and those on pPET were $pSUV_{max}$, pMTV, pTLG. The metabolic parameters that decreased after NICT were as follows: $\Delta SUV_{max} = bSUV_{max} - pSUV_{max}$, ΔMTV = bMTV - pMTV, and ΔTLG = bTLG - pTLG.

Pathological assessments

Pathological response was assessed by two experienced pathologists, who evaluated the percentage of residual viable tumor in the primary tumor resection using hematoxylin and eosin (HE) staining. The TRG was scored using a four-tiered grading system recommended by the American Joint Committee on Cancer/College of American Pathologists (AJCC/CAP) [8, 24]. The four-tiered grading system for TRG is as follows: grade 0 (TRG 0, complete response) = no residual viable cancer cells; grade 1 (TRG 1, moderate response) = only a small cluster or single residual viable cancer cells; grade 2 (TRG 2, minimal response) = residual cancer with desmoplastic response; grade 3 (TRG 3, poor response) = minimal evidence of tumor response. Grades 0 and 1 were classified as good response (GR), and Grades 2 and 3 were classified as poor response (PR). Other pathological data were also collected, including histological subtype, Lauren subtype, differentiation of tumor, and pathologic staging. Histological types were classified as poorly cohesive GC (PC) and other types of gastric cancer (non-PC), but signet-ring cell carcinoma was excluded in this study due to low ^{18}F-FDG uptake [25, 26].

Table 1 Characteristics of the 36 patients

Characteristic		Value Median (range) or *n* (%)
Age (years)		66 (35–77)
Gender	Female	13 (36.1)
	Male	23 (63.9)
Tumor location	Non-Antrum	18 (50)
	Antrum	18 (50)
Tumor differentiation	Moderate	14 (38.9)
	Poor	22 (61.1)
Histological type	PC	14 (38.9)
	Non-PC	22 (61.1)
Lauren type	Diffuse	19 (52.8)
	Intestinal	17 (47.2)
cT	cT_3	20 (55.6)
	cT_{4a}	16 (44.4)
cN	cN_{0-1}	20 (55.6)
	cN_{2-3}	16 (44.4)
pT	pT_{0-3}	26 (72.2)
	pT_4	10 (27.8)
pN	pN_{0-1}	24 (66.7)
	pN_{2-3}	12 (33.3)

Abbreviations: PC, poorly cohesive adenocarcinoma; Non-PC, other gastric cancer except for PC; *cT*, clinical T stage; cN, clinical N stage; pT, pathological T stage; pN, pathological *N* stage

Statistical analysis

Statistical analysis was performed with IBM SPSS version 26. Univariate analyses, including the Mann-Whitney U test, Kruskal-Wallis H test, and Crosstabs analyses were used to explore the association of both treatment effect and four-tiered TRG with all variables, continuous variables were expressed as median and range. Continuous variables were transferred into categorical variables according to median value. Multivariate analysis was further performed by binomial logistic regression analysis to identify independent and correlated factors of treatment effect and four-tiered TRG respectively. Receiver operating characteristic (ROC) curve analysis was used to evaluate the diagnostic performance and to determine the optimal cut-off value of the metabolic parameters to identify GR patients and TRG 0 after NICT. The DeLong test was utilized to assess the differences in the area under the ROC curve (AUC) among various metabolic parameters. Meanwhile, the McNemar test was employed to compare the differences in sensitivity and specificity between these metabolic parameters. And to

Table 2 Characteristics of the GR and PR groups

Factors	Response to treatment		Univariate analysis		Multivariate analysis		
	GR (*n* = 13)	PR (*n* = 23)	H/χ	*P* value	OR	95%CI	*P* value
$bSUV_{max}$	6.48 (3.28-20)	5.1 (2.99–11.02)	0.46	0.649	-	-	-
bMTV	20.47 (0.19-109.65)	28.39 (0.6-193.53)	0.91	0.379	-	-	-
bTLG	75.85 (0.58-642.55)	97.23 (1.65–652.2)	0.69	0.558	-	-	-
$pSUV_{max}$	3.38 (2.36–3.97)	3.96 (2.65–5.07)	7.25	0.474	-	-	-
pMTV[1]	0.97 (0.02–3.92)	3.43 (0.04–78.99)	2.11	0.036*	1.452	0.779–2.64	0.221
pTLG[2]	2.67 (0.05–12.15)	10.06 (0.11-240.92)	2.11	0.036*	1.135	0.93–1.384	0.213
ΔSUV_{max}	3.09 (-0.04-17.35)	1.61 (-0.35-6.98)	1.14	0.267	-	-	-
ΔMTV	19.46 (-0.24-109.63)	22.95 (-11.07-193.33)	0.148	0.879	-	-	-
ΔTLG	72.92 (-0.24-642.5)	83.26 (-36.53-651.7)	0.08	0.948	-	-	-
Age	67 (43–77)	65 (35–75)	0.99	0.328	-	-	-
Gender							
Female	3	10	1.498	0.221	-	-	-
Male	10	13					
Tumor location							
Non-Antrum	5	13	1.084	0.298	-	-	-
Antrum	8	10					
Tumor differentiation							
Moderate	6	8	0.452	0.501	-	-	-
Poor	7	15					
Histological type							
PC	2	12	4.73	0.030*	2.853[1] 0.438[2]	0.191-42.713[1] 0.195-43.501[2]	0.448[1] 0.438[2]
Non-PC	11	11					
Lauren type							
Diffuse	5	14	1.673	0.196	-	-	-
Intestinal	8	9					
cT							
cT3	10	10	3.763	0.052	-	-	-
cT4a	3	13					
cN							
cN0-1	10	10	3.763	0.052	-	-	-
cN2-3	3	13					
pT							
pT_{0-3}	12	14	4.092	0.043*	5.429[1] 5.451[2]	0.552-53.407[1] 0.552-53.777[2]	0.147[1] 0.147[2]
pT_4	1	9					
pN							
pN_{0-1}	11	13	2.95	0.086	-	-	-
pN_{2-3}	2	10					

Notes: 1, multivariate analysis for pMTV, histological type and pT; 2, multivariate analysis for pTLG, histological type and pT

Abbreviations: GR, good response to neoadjuvant immunochemotherapy; PR, poor response to neoadjuvant immunochemotherapy; OR, Odds Ratio. CI, confidence interval; $bSUV_{max}$, maximum standardized uptake value of bPET; bMTV, metabolic tumor volume of bPET; bTLG, total lesion glycolysis of bPET; $pSUV_{max}$, maximum standardized uptake value of pPET; pMTV, metabolic tumor volume of pPET; pTLG, total lesion glycolysis of pPET; ΔSUV_{max}, $bSUV_{max}$ - $pSUV_{max}$; ΔMTV, bMTV– pMTV; ΔTLG = bTLG - pTLG

control the risk of false positives arising from multiple comparisons, the Bonferroni correction was applied in pairwise analyses. All tests were two-sided and the statistical significance was set at $p < 0.05$.

Results

Patient characteristics

Forty-eight LAGC patients had both bPET and pPET at our center from August 2019 to October 2020. Out of these 48 patients, 12 patients were excluded, including 6 patients with different or unknown neoadjuvant chemotherapy, one patient with secondary malignancy, 3 patients with significant physiological uptake in the gastric wall, which affected the measurement of lesion uptake, 2 patients with an unfilled gastric cavity due to severe pyloric obstruction. Eventually, 36 eligible patients were enrolled in this study (Fig. 1). They received three cycles of sintilimab plus CapeOx and underwent both bPET and pPET. Their clinical characteristics are shown in Table 1. These patients had a median age of 66 years

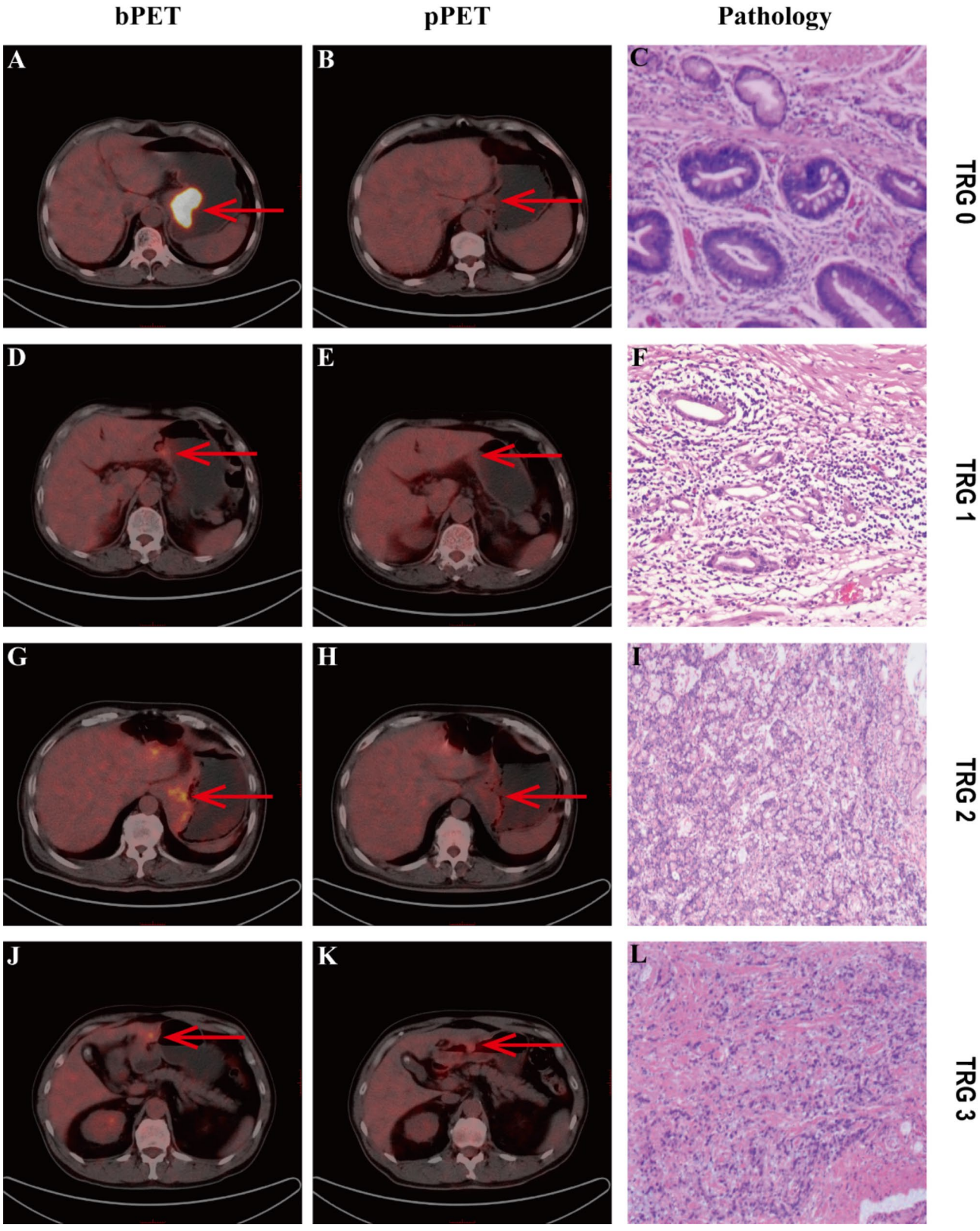

Fig. 2 (See legend on next page.)

(See figure on previous page.)

Fig. 2 ^{18}F-FDG PET/CT images and pathology obtained from TRG 0 to 3 respectively. (**A**-**C**) A 63-year-old male patient. **(A)** PET/CT before NICT, lesion located in cardia of the stomach with high ^{18}F-FDG uptake (SUV_{max}: 15.35, MTV: 79.74, TLG: 493.59); **(B)** PET/CT after NICT, ^{18}F-FDG uptake was significantly reduced (SUV_{max}: 3.97, MTV: 3.92, TLG: 12.15). **(C)** TRG of the lesion was classified as grade 0 (×400). (**D**-**F**) A 73-year-old male patient. **(D)** PET/CT before NICT, lesion located in antrum of the stomach with moderate ^{18}F-FDG uptake (SUV_{max}: 4.13, MTV: 2.94, TLG: 8.88); **(E)** PET/CT after NICT, ^{18}F-FDG uptake was slightly reduced (SUV_{max}: 3.97, MTV:< 2.5, TLG: NA). **(F)** TRG of the lesion was classified as grade 1 (×400). (**G**-**I**) A 73-year-old male patient. **(G)** PET/CT before NICT, lesion located in cardia of the stomach with moderate ^{18}F-FDG uptake (SUV_{max}: 5.67, MTV: 172.73, TLG: 551.26); **(H)** PET/CT after NICT, ^{18}F-FDG uptake was slightly reduced (SUV_{max}: 4.28, MTV: 38.38, TLG: 113.07). **(I)** TRG of the lesion was classified as grade 2 (×400). (**J**-**L**) A 73-year-old male patient. **(J)** PET/CT before NICT, lesion located in antrum of the stomach with moderate ^{18}F-FDG uptake (SUV_{max}: 4.5, MTV: 14.98, TLG: 42.54); **(K)** PET/CT after NICT, ^{18}F-FDG uptake was slightly reduced (SUV_{max}: 4.12, MTV: 14.31, TLG: 42.93). **(L)** TRG of the lesion was classified as grade 3 (×400)

old (range: 35–77), and 23 (63.9%) patients were male, 13 (36.1%) patients were female. The tumor locations were as follows: non-antrum (cardia or corpus) ($n = 18$, 50%) and antrum ($n = 18$, 50%); For tumor differentiation, 14 (38.9%) patients had moderate differentiation, 22 (61.1%) patients had poor differentiation. For histological type, there were 14 (38.9%) patients with poorly cohesive adenocarcinoma (PC) and 22 (61.1%) patients with other types of gastric cancer except for PC (non-PC). For Lauren type, there were 19 (52.8%) patients with diffuse-type gastric cancer and 17 (47.2%) patients with intestinal-type GC. The clinical T stage (cT) before NICT was as follows: cT_3 ($n = 20$, 55.6%) and cT_{4a} ($n = 16$, 44.4%), the clinical N stage (cN) were as follows: cN_{0-1} ($n = 20$, 55.6%), cN_{2-3} ($n = 16$, 44.4%), respectively. Their pathology T stage (pT) and pathology N stage (pN) were as follows: pT_{0-3} ($n = 26$, 72.2%), pT_4 ($n = 10$, 27.8%), pN_{0-1} ($n = 24$, 66.7%), pN_{2-3} ($n = 12$, 33.3%). There were no significant differences of many many variables in baseline characteristics between the GR group and the PR group, including age, gender, tumor location, differentiation type of GC, Lauren type of GC and stage (cT, cN, pN), except for histological type of GC ($p = 0.030$) and pT ($p = 0.043$) (Table 2). Similarly, for the TRG 0 group and the TRG 1–3 group, only Lauren type ($p = 0.016$), cT ($p = 0.041$), and cN ($p = 0.041$) were significantly different (Table 4).

However, in multivariate analysis, when integrated with histopathological type and cT in binomial logistic regression analysis, neither pMTV (odds ratio (OR) = 1.452, 95% confidence interval (CI): 0.779–2.64, $p = 0.221$) nor pTLG (OR = 1.135, 95% CI: 0.93–1.384, $p = 0.213$) showed significant differences (Table 2). Given the nature of the four-tiered TRG groups, ordinal logistic regression was deemed inappropriate for the analysis. Instead, binomial logistic regression analyses were performed based on the results of the univariate analysis of the TRG 0 and TRG 1–3 groups. When integrated with ΔSUV_{max}, ΔTLG, cT and Lauren type, both ΔSUV_{max} and ΔTLG were non-significant, with OR = 1.24, 95%CI: 0.822–1.868, $p = 0.305$ and OR = 1, 95%CI: 0.991–1.009, $p = 0.969$, respectively (Table 4).

Pathological response to NICT

According to the four-tiered grading system recommended by the AJCC/CAP, the histopathological analysis revealed that 13 (36.1%) patients had GR to NICT, including 5 (13.9%) patients with TRG 0 and 8 (22.2%) patients with TRG 1, while 23 (63.9%) patients were PR, including 20 (55.6%) patients with TRG 2 and 3 (8.3%) patients with TRG 3 (Fig. 2).

Correlation between PET/CT metabolic and pathological response after NICT

Univariate analysis demonstrated that pMTV and pTLG in the GR group were significantly lower than those in the PR group (0.97: [0.02–3.92] vs. 3.43: [0.04–78.99], and 2.67: [0.05–12.15] vs. 10.06: [0.11-240.92], $p = 0.036$ for both). However, there was no significant difference in $bSUV_{max}$, bMTV, bTLG, $pSUV_{max}$, ΔSUV_{max}, ΔMTV, and ΔTLG between the GR and PR groups (Table 2; Fig. 3). The ROC curve analyses provided the optimal cutoff values of PET/CT parameters for distinguishing the GR and PR groups (Table 5; Fig. 5A). With the identified cutoff values of pMTV and pTLG at 1.68 cm^3 (AUC = 0.683) and 4.71 cm^3 (AUC = 0.683), the sensitivity, specificity, accuracy, positive predictive value, and negative predictive value were 68.8%, 80.0%, 73.1%, 84.6%, and 61.5%, respectively. DeLong test and McNemar test showed no significant difference in their AUC, sensitivity, or specificity ($p > 0.05$).

Notably, results of this study showed that pMTV and pTLG in the GR group were significantly lower compared to the PR group. However, the area under the ROC curve was less than satisfactory, and Fig. 3 illustrates that the data within each group exhibited considerable variability. Given the limited value of PET/CT metabolic parameters in distinguishing between the GR and PR groups, it is meaningful to further investigate the differences in PET/CT metabolic parameters among the four-tiered TRG groups. In terms of TRG, univariate analysis showed that $bSUV_{max}$, bMTV, bTLG, ΔSUV_{max}, ΔMTV, and ΔTLG in the TRG 0 group were higher than those in the TRG 1–3 groups. However, statistical differences were found only between the TRG 0 and TRG 1 groups after Post Hoc Multiple Comparisons (all $p < 0.05$) (Table 3; Fig. 4). The values were as follows: TRG 0 (11.95: [8.06-20] in $bSUV_{max}$, 59.39: [26.57-109.65] in bMTV, 324.86: [107.87-642.55] in bTLG, 8.79: [4.83–17.35] in ΔSUV_{max}, 57.42: [25.94-109.63] in ΔMTV, 318.76: [105.94–642.5] in ΔTLG) vs. TRG 1 (4.52: [3.28–12.63] in $bSUV_{max}$; 11.77:

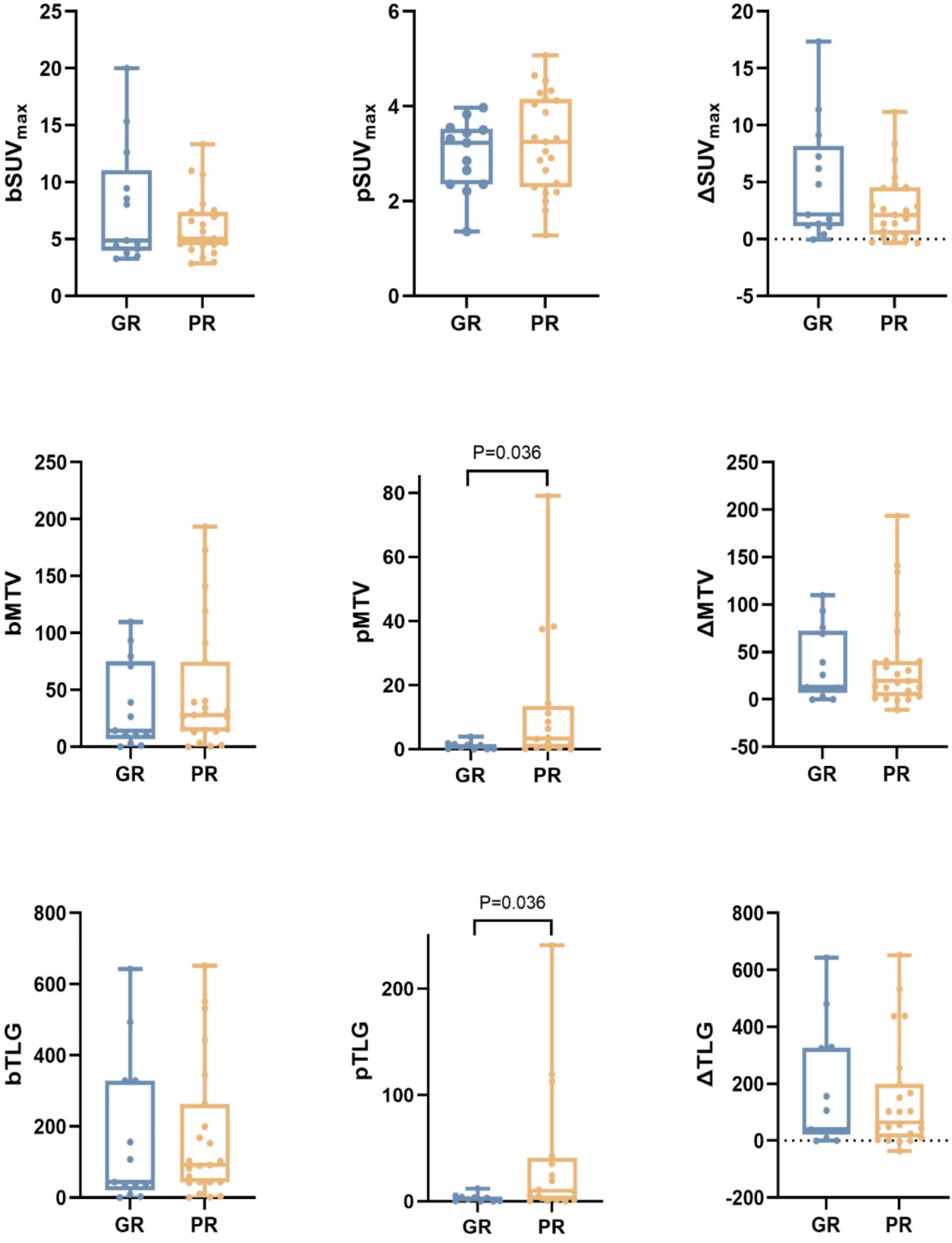

Fig. 3 Box-plot of metabolic parameters of primary lesions in the GR and PR groups. pMTV and pTLG in the GR group were significantly lower than those in the PR group ($p = 0.036$ for both), there was no significant difference in bSUV$_{max}$, bMTV, bTLG, pSUV$_{max}$, ΔSUV$_{max}$, ΔMTV, and ΔTLG between the GR and PR groups. Abbreviations: GR, good response; PR, poor response

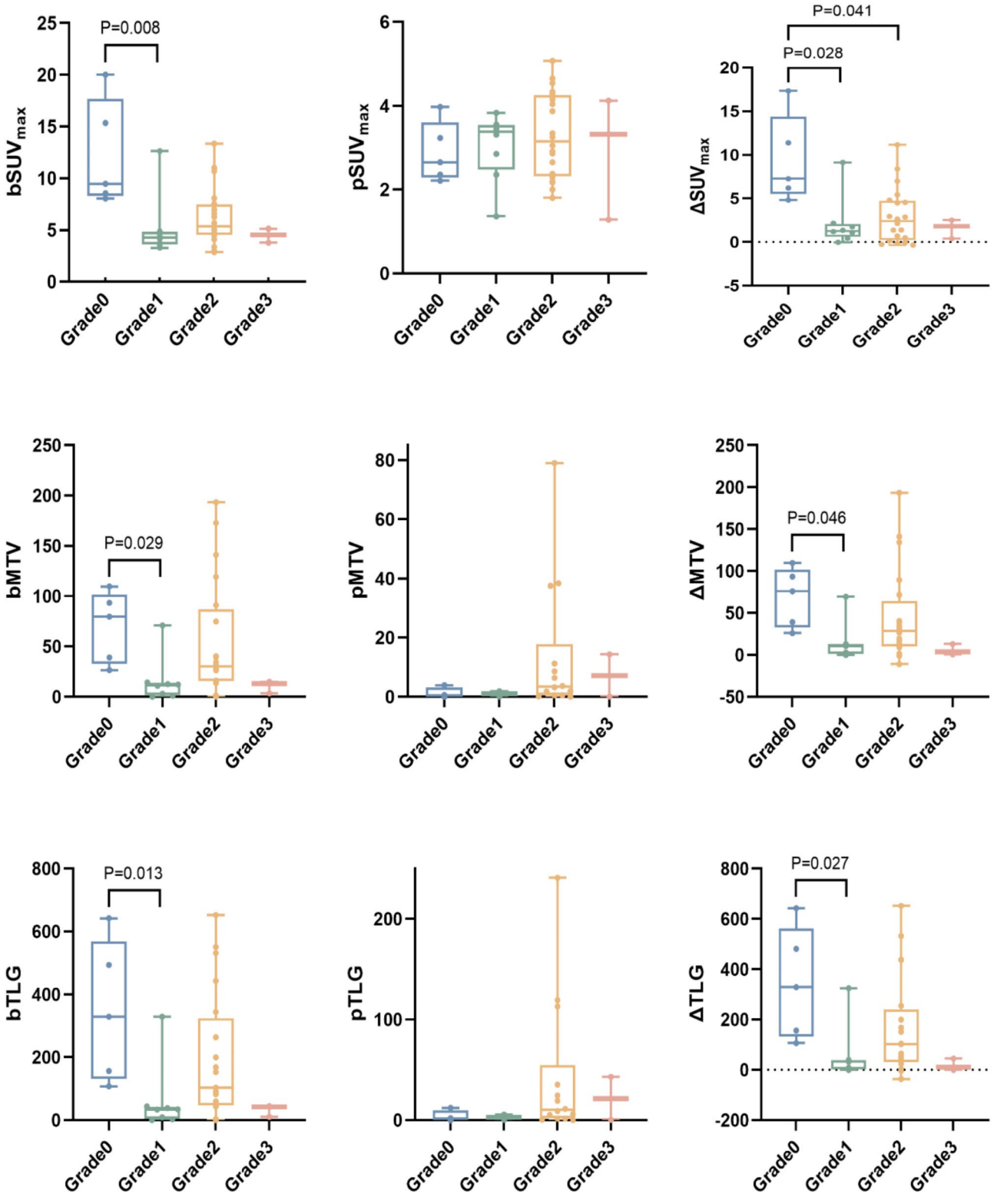

Fig. 4 Box-plot of metabolic parameters of primary lesions according to TRG grade groups. bSUV$_{max}$, bMTV, bTLG, ΔSUV$_{max}$, ΔMTV, and ΔTLG in the TRG 0 group were higher than those in the TRG 1–3 groups. Statistical differences were only found between the TRG 0 and the TRG 1 group (all $p < 0.05$). Additionally, ΔSUV$_{max}$ of the TRG 0 group was higher than that of the TRG 2 group

[0.19–70.97] in bMTV; 35.95: [0.58-328.88] in bTLG; 1.15: [-0.04-9.13] in ΔSUV$_{max}$; 10.72: [-0.24-69.4] in

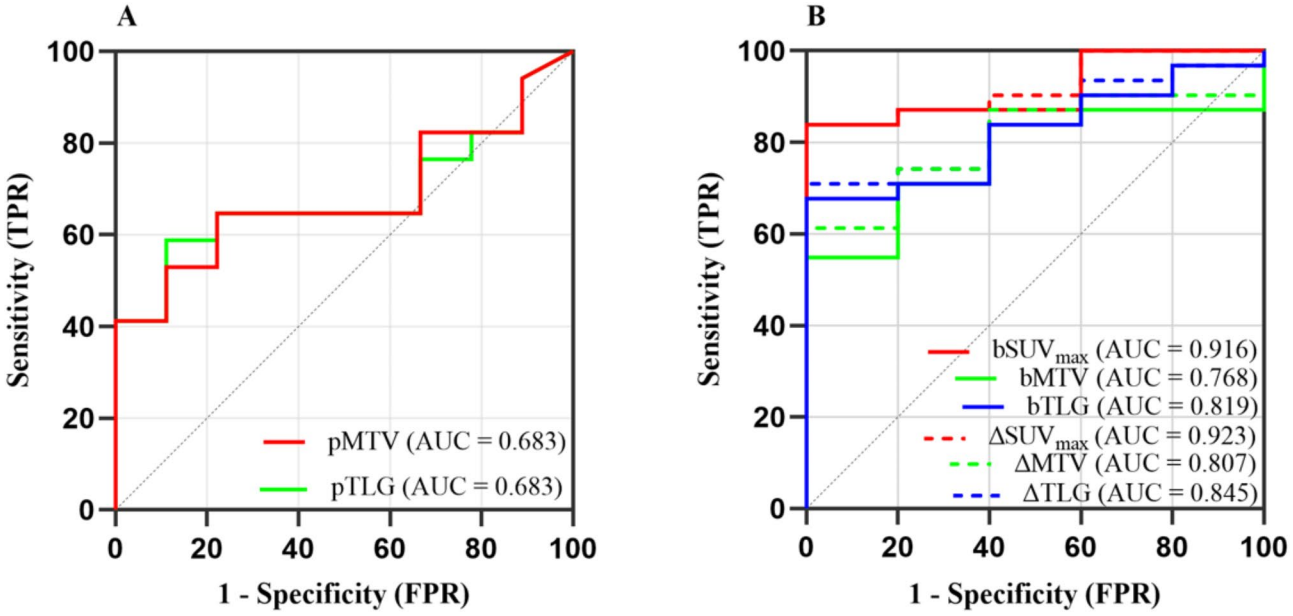

Fig. 5 ROC curve analyses for treatment effect and four-tiered TRG.. **A**, ROC curve for pMTV and pTLG of PET against the GR and PR groups. When the identified cutoff values of pMTV and pTLG were 1.68 cm^3 (AUC = 0.683) and 4.71 cm^3 (AUC = 0.683), respectively, the sensitivity, specificity, accuracy, positive predictive value, and negative predictive value were 68.8%, 80.0%, 73.1%, 84.6%, and 61.5%, respectively. **B**, ROC curve for SUV_{max}, MTV and TLG of baseline PET and the changes against the TRG 0 group. When the identified cutoff values were $bSUV_{max}$ = 7.8 (AUC = 0.916), bMTV = 36.76 cm^3 (AUC = 0.768), bTLG = 105.55 cm^3 (AUC = 0.819), ΔSUV_{max}= 4.82 (AUC = 0.923), ΔMTV = 22.64 cm^3 (AUC = 0.807), ΔTLG = 104.71 cm^3 (AUC = 0.845) respectively, and with high sensitivity (80.0% for bMTV, and 100% for others), specificity (83.9%, 71.0%, 67.7%, 83.9%, 61.3% and 71.0%), accuracy (86.1%, 66.7%, 72.2%, 86.1%, 66.7% and 75.0%), positive predictive value (50.0%, 23.1%, 33.3%, 50.0%, 29.4%, 35.7%), negative predictive values (91.3% for bMTV, and 100% for others). Abbreviations: ROC, receiver operating characteristic, AUC, area under curve

ΔMTV; 32.91: [-0.24-324.6] in ΔTLG). The optimal cutoff values identified on ROC analysis of ^{18}F-FDG PET/CT parameters for predicting pathological TRG 0 group were as follows: $bSUV_{max}$ = 7.8 (AUC = 0.916), bMTV = 36.76 cm^3 (AUC = 0.768), bTLG = 105.55 cm^3 (AUC = 0.819), ΔSUV_{max}= 4.82 (AUC = 0.923), ΔMTV = 22.64 cm^3 (AUC = 0.807), ΔTLG = 104.71 cm^3 (AUC = 0.845) respectively, and with high sensitivity(80.0% for bMTV, and 100% for others), specificity (83.9%, 71.0%, 67.7%, 83.9%, 61.3% and 71.0%), accuracy (86.1%, 66.7%, 72.2%, 86.1%, 66.7% and 75.0%), positive predictive value (50.0%, 23.1%, 33.3%, 50.0%, 29.4%, 35.7%), negative predictive value (91.3% for bMTV, and 100% for others) (Table 5; Fig. 5B). The DeLong test and McNemar test revealed no significant differences in their AUC, sensitivity, or specificity ($p > 0.05$), despite an apparent trend toward differences observed in Fig. 5B.

Discussion

GC patients are frequently diagnosed with LAGC at their initial visit [27]. NICT has emerged as a promising NAT strategy for LAGC, demonstrating potential in promoting tumor regression [7, 28]. Achieving a pathological complete response (pCR) following NAT before surgery is a crucial factor in improving survival rates [4, 5]. While ^{18}F-FDG PET/CT has been extensively used to evaluate the efficacy of NAT in solid tumors, its application in assessing the efficacy of NICT in LAGC remains fraught with challenges and is a subject of skepticism [10, 11, 20, 29]. Additionally, there is a notable scarcity of relevant studies in this specific context. Thus, we aim to identify imaging biomarkers of bPET and pPET in LAGC patients to predict pathological response to NICT before surgery.

Initially, we identified that among various ^{18}F-FDG PET/CT imaging metabolic parameters, lower pMTV and pTLG might serve as potential imaging biomarkers for predicting GR patients. However, the accuracy was unsatisfactory (AUC = 0.683 for both). Upon further analysis of the four-tiered TRG groups, instead of pMTV and pTLG, $bSUV_{max}$, bMTV, bTLG, ΔSUV_{max}, ΔMTV, and ΔTLG demonstrated superior diagnostic accuracy (AUC = 0.916, 0.768, 0.819, 0.923, 0.807, and 0.845 respectively) for the TRG 0 group, and their diagnostic accuracy showed no difference after DeLong test. The results suggested that a high FDG uptake prior to NICT, a low FDG uptake post-NICT, and a substantial decrease in FDG uptake in the primary tumor after NICT are indicators for favorable response to NICT. Limited research has been conducted on using ^{18}F-FDG PET/CT to assess the pathological response to NAT in GC, and yielding inconsistent outcomes [13, 16, 30, 31]. Mi L. et al. [13] noted that FDG uptake post NAT and the percentage

Table 3 The characteristics of PET/CT parameters in four-tiered TRG groups

Factors Median (Range)	TRG				Univariate analysis	
	Grade 0	Grade 1	Grade 2	Grade 3	Z	*P* value
$bSUV_{max}$	11.95(8.06-20)	4.52(3.28–12.63)	5.36 (2.99–11.02)	4.82(4.5–5.14)	11.24	0.01*
bMTV	59.39 (26.57-109.65)	11.77 (0.19–70.97)	30.07 (0.6-193.53)	13.99 (13-14.98)	11.3	0.01*
bTLG	324.86 (107.87-642.55)	35.95 (0.58-328.88)	102.95 (1.65–652.2)	43.57(42.54–44.59)	11.9	0.008*
$pSUV_{max}$	2.94 (2.36–3.97)	3.47 (2.85–3.83)	4 (2.65–5.07)	3.72 (3.32–4.12)	0.91	0.824
pMTV	0.325 (0.02–3.92)	1.35 (0.09–1.91)	3.43 (0.04–78.99)	7.2 (0.08–14.31)	4.95	0.176
pTLG	0.99 (0.05–12.15)	3.67 (0.32–5.54)	10.06 (0.11-240.92)	21.59 (0.25–42.93)	4.95	0.176
ΔSUV_{max}	8.79 (4.83–17.35)	1.15 (-0.04-9.13)	1.77 (-0.35-6.98)	1.1 (0.38–1.82)	0.95	0.024*
ΔMTV	57.42 (25.94-109.63)	10.72 (-0.24-69.4)	28.64 (-11.07-193.33)	6.8 (0.67–12.92)	9.47	0.024*
ΔTLG	318.76 (105.94–642.5)	32.91 (-0.24-324.6)	102.13 (-36.53-651.7)	21.98 (-0.39-44.34)	10.64	0.014*

Abbreviations: TRG, tumor regression grade

changes in FDG uptake were correlated with pathological response. Consistent with this finding, Ott K. et al. [31] also indicated that the percentage changes in FDG uptake were associated with pathological response to NAT. However, The contrastive analysis of ^{68}Ga-FAPI-04 and ^{18}F-FDG PET/CT indicated that FAPI uptake was linked to pathological remission following NAT, whereas FDG uptake is not [32]. Additionally, the study by Morgagni P. et al. suggested that ^{18}F-FDG PET/CT had limited usefulness in predicting pathological response [16]. In a study focusing on gastroesophageal junction adenocarcinoma, it was indicated that a reduction in SUV_{max} of less than 35% was strongly correlated with the absence of pathological response following NAT [15]. These discrepancies may be influenced by a variety of factors, with the particularity of gastric cancer being a significant reason [17, 33]. The FDG uptake in gastric cancer is associated with multiple factors, including the location and size of the lesion, the pathological histological type and degree of differentiation, and the physiological uptake of the gastric wall itself. On a molecular level, the interplay between FDG uptake in gastric cancer and factors like glucose transporters (GLUT) expression and hypoxia is intricate and multifaceted [10, 11, 18]. Moreover, the treatment regimen also serves as a crucial influencing factor. In the aforementioned previous studies, few have managed to contral these aforementioned influencing factors.

In this study, the treatment regimen employed was NICT. This was a main factor that accounts for the discrepancies between the results of this study and those of previous studies. Currently, there was limited research on using ^{18}F-FDG PET/CT to predict the pathological response to NICT in LAGC. To our knowledge, this may be the first pilot study of its kind. In this context, we draw an analogy with the existing research on ESCC, two studies on ESCC have demonstrated that post-NICT scan parameters and their changes were significantly associated with the pathological response [21, 22]. The role of immunotherapy in tumor treatment is becoming increasingly significant [7, 27, 28]. Evaluating the efficacy of immunotherapy presents a substantial challenge. Immunotherapy mechanisms restore the body's normal anti-tumor immune response through re-initiating and sustaining the tumor-immune cycle, thereby control and eliminate the tumor [6]. Traditional imaging assessments may confounded by pseudo-progression, hyperprogression, and delayed progression, which both offer opportunities and pose challenges for ^{18}F-FDG PET/CT in assessing the efficacy of immunotherapy [9–11, 19]. One case reported demonstrated pseudo-progression on ^{18}F-FDG PET [20], while another case reported showed that PET was performed both before and after NICT, indicating a response that was subsequently confirmed by pathology [29]. Although some studies have indicated a positive correlation between PD-L1 expression and FDG uptake in GC, the relationship between immunotherapy and the tumor microenvironment is complex [6, 11, 19]. Therefore, the correlation between PD-L1 expression and FDG uptake remains a topic of ongoing debate. Due to the retrospective nature of this study, we were unable to determine the PD-L1 expression levels in gastric cancer tissue pathology.

Prior research has shown that several factors influence the visibility of ^{18}F-FDG PET/CT in GC and affect the application of baseline PET in LAGC [18, 33–35]. FDG avidity is dependent on tumor histologic subtype, with low FDG uptake more frequently observed in diffuse-type histology (mucinous, signet ring, and poorly differentiated) compared to the intestinal subtype. The SUV_{max} of ^{18}F-FDG PET/CT is significantly correlated with tumor size, and lower FDG uptake is often found in early GC, likely due to fewer total cancer cells in the primary lesions. The motility and physiological uptake of FDG in the stomach also impact the accuracy of PET/CT in diagnosing gastric cancer. In partial alignment with previous studies, univariate analyses in our research indicated that histopathological type and cT were associated with the GR and PR groups, while cT and Lauren type

Table 4 Characteristics of the TRG 0 and TRG 1–3 groups

Factors	Response to treatment		Univariate analysis		Multivariate analysis		
	TRG 0 ($n=5$)	TRG 1–3 ($n=31$)	H/χ	*P* value	OR	95%CI	*P* value
$bSUV_{max}$	11.95(8.06-20)	4.72 (2.99–12.63)	2.951	0.001*	-	-	-
bMTV	59.39 (26.57-109.65)	16.05 (0.19-193.53)	1.898	0.046*	-	-	-
bTLG	324.86 (107.87-642.55)	59.87 (0.58–652.2)	2.264	0.021*	-	-	-
$pSUV_{max}$	2.94 (2.36–3.97)	3.31 (2.65–5.07)	0.801	0.448	-	-	-
pMTV	0.325 (0.02–3.92)	1.85 (0.04–78.99)	1.564	0.130			
pTLG	0.99 (0.05–12.15)	5.34 (0.11-240.92)	1.564	0.130			
ΔSUV_{max}	8.79 (4.83–17.35)	1.77 (-0.04-9.13)	2.996	0.001*	1.24	0.822–1.868	0.305
ΔMTV	57.42 (25.94-109.63)	12.98 (-0.24-193.33)	2.173	0.028*	-	-	-
ΔTLG	318.76 (105.94–642.5)	44.34 (-0.24-651.7)	2.447	0.012*	1	0.991–1.009	0.969
Age	66 (63–77)	66 (35–75)	0.963	0.348	-	-	-
Gender							
Female	0	13	3.282	0.136	-	-	-
Male	5	18					
Tumor location							
Non-Antrum	3	15	0.232	1	-	-	-
Antrum	2	16					
Tumor differentiation							
Moderate	3	11	1.089	0.357	-	-	-
Poor	2	20					
Histological type							
PC	0	14	3.695	0.134	-	-	-
Non-PC	5	17					
Lauren type							
Diffuse	0	19	6.49	0.016*	0	0	0.998
Intestinal	5	12					
cT							
cT3	5	15	4.645	0.041*	0	0	0.998
cT4a	0	16					
cN							
cN0-1	5	15	4.645	0.041*	-	-	-
cN2-3	0	16					
pT							
pT_{0-3}	4	22	0.175	1	-	-	-
pT_4	1	9					
pN							
pN_{0-1}	4	20	0.465	0.646	-	-	-
pN_{2-3}	1	11					

Note: Several parameters were excluded from the multivariate analysis owing to issues of collinearity

were linked to the four-tiered groups. However, some studies have shown no correlation between the Lauren type and lesion site with SUVmax, possibly due to small sample sizes. Signet ring cell carcinoma was excluded from our study population primarily due to its low FDG uptake characteristics, which are affected by the physiological uptake of the gastric wall itself or often have an SUV_{max} below 2.5, its unique biological behavior, and its distinctive immune microenvironment features, thus, necessitating separate analysis [25, 26, 33]. The limited sample size of this study precluded detailed subgroup analyses and control for influencing factors such as T stage, histopathological type, and Lauren type. In this study, all patients received the same treatment regimen, which represents the most significant advantage of this study. However, this approach resulted in a small sample size, which is the most substantial drawback of this study. As can be seen from Tables 2, 3 and 4; Figs. 3 and 4, there was considerable dispersion in our data. Therefore, our findings require further confirmation through large-scale studies.

This study has several limitations. First, it was a pilot study, characterized by its retrospective, single-center, and small-sample nature, with dispersed data, thus future studies with larger sample sizes are required to further validate our findings. Second, due to the small sample

Table 5 Cut-off values of metabolic parameters on predicting efficacy of PR and TRG 0

	Cut-off	AUC (95%CI)	SE%	SP%	ACC%	PPV%	NPV%
Predicting for PR							
pMTV	1.68	0.683 (0.479–0.887)	68.8	80.0	73.1	84.6	61.5
pTLG	4.71	0.683 (0.478–0.887)	68.8	80.0	73.1	84.6	61.5
Predicting for TRG 0							
$bSUV_{max}$	7.80	0.916 (0.819-1.000)	100.0	83.9	86.1	50.0	100.0
bMTV	36.76	0.768 (0.603–0.933)	80.0	71.0	66.7	23.1	91.3
bTLG	105.55	0.819 (0.673–0.966)	100.0	67.7	72.2	33.3	100.0
ΔSUV_{max}	4.82	0.923 (0.831-1.000)	100.0	83.9	86.1	50.0	100.0
ΔMTV	22.64	0.807 (0.655–0.958)	100.0	61.3	66.7	29.4	100.0
ΔTLG	104.71	0.845 (0.709–0.981)	100.0	71.0	75.0	35.7	100.0

Abbreviations: AUC, area under the cure; SE, sensitivity; SP, specificity; ACC, accuracy; NPV, negative predictive value; PPV, positive predictive

size, we could not conduct detailed research, such as subgroup analysis of different histological types of GC. Third, due to its retrospective nature, we could not obtain the expression of PD-1 and could not conduct correlation studies with metabolic parameters.

Conclusion

Imaging biomarkers derived from the combination of baseline ^{18}F-FDG PET/CT and post-treatment ^{18}F-FDG PET/CT demonstrated significant potential in predicting the pathological response to NICT in LAGC patients before surgery. These metabolic parameters can be integrated into clinical practice to facilitate more informed surgical planning and therapeutic decision-making, and it is still considered appropriate to endorse the routine application of both baseline ^{18}F-FDG PET/CT and post-treatment ^{18}F-FDG PET/CT imaging in NICT-treated LAGC patients prior to radical surgery. While caution is warranted in interpreting the data due to the limited sample size in this study, validation of these results necessitates expanding the sample size.

Abbreviations

bPET	baseline PET/CT
pPET	post-treatment PET/CT
TRG	tumor regression grade
NICT	neoadjuvant immunochemotherapy
SUV_{max}	maximum standardized uptake value
MTV	metabolic tumor volume
TLG	total lesion glycolysis
NA	Not Available

Acknowledgements

Not applicable.

Author contributions

Mimi Xu: Conceptualization, draw ROI on 18 F-FDG PET/CT, and wrote the main manuscript text. Yafei Zhang: Conceptualization and draw ROI on 18 F-FDG PET/CT. Kui Zhao: Evaluate the quality of 18 F-FDG PET/CT scans. Haiping Jiang: Assess the clinical status of patients. Guangfa Wang: Preparation and quality assurance of radiopharmaceuticals. Yan Wu: Image acquisition. Yu Wang: Prepared figures and tables. Nian Liu: Edited the manuscript. Xinhui Su: Reviewed and edited the manuscript.

Funding

This study was supported by the National Key Research and Development Program of China (2023YFF0716000), National Natural Science Foundation of China (82472013, 82071965), Major plan of Jointly Constructed project by the Science and Technology Department of the State Administration of Traditional Chinese Medicine and the Zhejiang Provincial Administration of Traditional Chinese Medicine (GZY-ZJ-KJ-24025), and National High Performance Medical Device Innovation Center Innovation Fund (NMED2024CX-01-002).

Data availability

The datasets used and/or analyzed during the current study are available from the corresponding author upon reasonable request.

Declarations

Ethics approval and consent to participate

The data collection and the methods used in this study were carried out in accordance with the ethical standards of the institutional and national research committee and with the 1964 Helsinki Declaration and its later amendments or comparable ethical standards. The data collection program for this study was approved by Clinical Research Ethics Committee of the First Affiliated Hospital of Zhejiang University School of Medicine (No.20230569) with a waiver for individual informed consent for this retrospective study.

Consent for publication

Not applicable.

Competing interests

The authors declare no competing interests.

Author details

[1]Department of Nuclear Medicine, The First Affiliated Hospital, Zhejiang University School of Medicine, Hangzhou 310003, China
[2]Oncology Department, The First Affiliated Hospital, Zhejiang University School of Medicine, Hangzhou 310003, China
[3]The Second Affiliated Hospital of Zhejiang Chinese Medical University, Hangzhou 310005, China

Received: 25 November 2024 / Accepted: 18 February 2025
Published online: 28 February 2025

References

1. Smyth EC, Nilsson M, Grabsch HI, van Grieken NC, Lordick F. Gastric cancer. Lancet. 2020;396(10251):635–48.
2. Bray F, Ferlay J, Soerjomataram I, Siegel RL, Torre LA, Jemal A. Global cancer statistics 2018: GLOBOCAN estimates of incidence and mortality worldwide for 36 cancers in 185 countries. CA Cancer J Clin. 2018;68(6):394–424.
3. Zou ZH, Zhao LY, Mou TY, Hu YF, Yu J, Liu H, Chen H, Wu JM, An SL, Li GX. Laparoscopic vs open D2 gastrectomy for locally advanced gastric cancer: a meta analysis. World J Gastroenterol. 2014;20(44):16750–64.

4. Fields RC, Strong VE, Gonen M, Goodman KA, Rizk NP, Kelsen DP, Ilson DH, Tang LH, Brennan MF, Coit DG, et al. Recurrence and survival after pathologic complete response to preoperative therapy followed by surgery for gastric or gastrooesophageal adenocarcinoma. Br J Cancer. 2011;104(12):1840–7.
5. Lin C, Ma J, Zhu C, Zhao X, Chen Y, Zang L, Liu F. Is pathologic complete response a good predictor for the Long-Term, clinical outcome in patients with gastric Cancer after neoadjuvant chemotherapy?? A retrospective, Multi-institution study in China. Ann Surg Oncol. 2023;30(9):5534–42.
6. Chen Y, Jia K, Sun Y, Zhang C, Li Y, Zhang L, Chen Z, Zhang J, Hu Y, Yuan J, et al. Predicting response to immunotherapy in gastric cancer via multi dimensional analyses of the tumour immune microenvironment. Nat Commun. 2022;13(1):4851.
7. Jing SW, Zhai C, Zhang W, He M, Liu QY, Yao JF, Wang R, Tian ZQ, Wang J, Liu JF. Comparison of neoadjuvant immunotherapy plus chemotherapy versus chemotherapy alone for patients with locally advanced esophageal squamous cell carcinoma: A propensity score matching. Front Immunol. 2022;13:970534.
8. Langer R, Becker K. Tumor regression grading of Gastrointestinal cancers after neoadjuvant therapy. Virchows Arch. 2018;472(2):175–86.
9. Wang W, Gao Z, Wang L, Li J, Yu J, Han S, Meng X. Application and prospects of molecular imaging in immunotherapy. Cancer Manag Res. 2020;12:9389–403.
10. Gao Y, Wu C, Chen X, Ma L, Zhang X, Chen J, Liao X, Liu M. PET/CT molecular imaging in the era of immune-checkpoint inhibitors therapy. Front Immunol. 2022;13:1049043.
11. Kaira K, Kuji I, Kagamu H. Value of (18)F-FDG-PET to predict PD-L1 expression and outcomes of PD-1 Inhibition therapy in human cancers. Cancer Imaging. 2021;21(1):11.
12. Wahl RL, Jacene H, Kasamon Y, Lodge MA. From RECIST to PERCIST: evolving considerations for PET response criteria in solid tumors. J Nucl Med. 2009;50(Suppl 1):S122–50.
13. Mi L, Zhao Y, Zhao X, Yin F, Yin X, Li N, Shi J, Han X, Duan X, Zhao M, et al. (18) F-Fluorodeoxyglucose positron emission tomography-Computed tomography metabolic parameters before and after neoadjuvant chemotherapy can predict the postoperative prognosis of locally advanced gastric cancer. Cancer Biother Radiopharm. 2021;36(8):662–71.
14. Sanchez-Izquierdo N, Perlaza P, Pages M, Buxo E, Rios J, Rubello D, Colletti PM, Mayoral M, Casanueva S, Fernandez-Esparrach G, et al. Assessment of response to neoadjuvant chemoradiotherapy by 18F-FDG PET/CT in patients with locally advanced esophagogastric junction adenocarcinoma. Clin Nucl Med. 2020;45(1):38–43.
15. Lordick F, Ott K, Krause BJ, Weber WA, Becker K, Stein HJ, Lorenzen S, Schuster T, Wieder H, Herrmann K, et al. PET to assess early metabolic response and to guide treatment of adenocarcinoma of the oesophagogastric junction: the MUNICON phase II trial. Lancet Oncol. 2007;8(9):797–805.
16. Morgagni P, Bencivenga M, Colciago E, Tringali D, Giacopuzzi S, Framarini M, Saragoni L, Mura G, Graziosi L, Marino E, et al. Limited usefulness of 18F-FDG PET/CT in predicting tumor regression after preoperative chemotherapy for noncardia gastric cancer: the Italian research group for gastric Cancer (GIRCG) experience. Clin Nucl Med. 2020;45(3):177–81.
17. Dassen AE, Lips DJ, Hoekstra CJ, Pruijt JF, Bosscha K. FDG-PET has no definite role in preoperative imaging in gastric cancer. Eur J Surg Oncol. 2009;35(5):449–55.
18. Yuan LW, Yamashita H, Seto Y. Glucose metabolism in gastric cancer: the cutting-edge. World J Gastroenterol. 2016;22(6):2046–59.
19. Borcoman E, Kanjanapan Y, Champiat S, Kato S, Servois V, Kurzrock R, Goel S, Bedard P, Le Tourneau C. Novel patterns of response under immunotherapy. Ann Oncol. 2019;30(3):385–96.
20. Lee Y, Won HS, Seo KJ, Na SJ. FDG PET images of pseudoprogression after Nivolumab-FOLFOX chemotherapy in a gastric Cancer patient. Clin Nucl Med. 2024;49(12):1139–41.
21. Wang S, Di S, Lu J, Xie S, Yu Z, Liang Y, Gong T. F-FDG PET/CT predicts the role of neoadjuvant immunochemotherapy in the pathological response of esophageal squamous cell carcinoma. Thorac Cancer. 2023;18(24):2338–49.
22. Wang X, Yang W, Zhou Q, Luo H, Chen W, Yeung SJ, Zhang S, Gan Y, Zeng B, Liu Z, et al. The role of (18)F-FDG PET/CT in predicting the pathological response to neoadjuvant PD-1 Blockade in combination with chemotherapy for resectable esophageal squamous cell carcinoma. Eur J Nucl Med Mol Imaging. 2022;49(12):4241–51.
23. Ji X, Bu ZD, Yan Y, Li ZY, Wu AW, Zhang LH, Zhang J, Wu XJ, Zong XL, Li SX, et al. The 8th edition of the American joint committee on Cancer tumor-node-metastasis staging system for gastric cancer is superior to the 7th edition: results from a Chinese mono-institutional study of 1663 patients. Gastric Cancer. 2018;21(4):643–52.
24. Tsagkalidis V, Blaszczyk MB, In H. Interpretation of tumor response grade following preoperative therapy for gastric cancer: an overview. Cancers (Basel) 2023, 15(14).
25. Nagtegaal ID, Odze RD, Klimstra D, Paradis V, Rugge M, Schirmacher P, Washington KM, Carneiro F, Cree IA, Board WHOCTE. The 2019 WHO classification of tumours of the digestive system. Histopathology. 2020;76(2):182–8.
26. Mariette C, Carneiro F, Grabsch HI, van der Post RS, Allum W, de Manzoni G. European chapter of international gastric Cancer A: consensus on the pathological definition and classification of poorly cohesive gastric carcinoma. Gastric Cancer. 2019;22(1):1–9.
27. Yeh JH, Yeh YS, Tsai HL, Huang CW, Chang TK, Su WC, Wang JY. Neoadjuvant chemoradiotherapy for locally advanced gastric cancer: where are we at? Cancers (Basel) 2022, 14(12).
28. Jiang H, Yu X, Li N, Kong M, Ma Z, Zhou D, Wang W, Wang H, Wang H, He K et al. Efficacy and safety of neoadjuvant sintilimab, oxaliplatin and capecitabine in patients with locally advanced, resectable gastric or gastroesophageal junction adenocarcinoma: early results of a phase 2 study. J Immunother Cancer 2022, 10(3).
29. Zhou ML, Xu RN, Tan C, Zhang Z, Wan JF. Advanced gastric cancer achieving major pathologic regression after chemoimmunotherapy combined with hypofractionated radiotherapy: A case report. World J Gastrointest Oncol. 2023;15(6):1096–104.
30. Schneider PM, Eshmuminov D, Rordorf T, Vetter D, Veit-Haibach P, Weber A, Bauerfeind P, Samaras P, Lehmann K. (18)FDG-PET-CT identifies histopathological non-responders after neoadjuvant chemotherapy in locally advanced gastric and cardia cancer: cohort study. BMC Cancer. 2018;18(1):548.
31. Ott K, Fink U, Becker K, Stahl A, Dittler HJ, Busch R, Stein H, Lordick F, Link T, Schwaiger M, et al. Prediction of response to preoperative chemotherapy in gastric carcinoma by metabolic imaging: results of a prospective trial. J Clin Oncol. 2003;21(24):4604–10.
32. Miao Y, Feng R, Yu T, Guo R, Zhang M, Wang Y, Hai W, Shangguan C, Zhu Z, Li B. Value of (68)Ga-FAPI-04 and (18)F-FDG PET/CT in early prediction of pathologic response to neoadjuvant chemotherapy in locally advanced gastric Cancer. J Nucl Med. 2024;65(2):213–20.
33. Kaneko Y, Murray WK, Link E, Hicks RJ, Duong C. Improving patient selection for 18F-FDG PET scanning in the staging of gastric cancer. J Nucl Med. 2015;56(4):523–9.
34. Jayaprakasam VS, Paroder V, Schoder H. Variants and pitfalls in PET/CT imaging of Gastrointestinal cancers. Semin Nucl Med. 2021;51(5):485–501.
35. Takebayashi R, Izuishi K, Yamamoto Y, Kameyama R, Mori H, Masaki T, Suzuki Y. [^{18}F]Fluorodeoxyglucose accumulation as a biological marker of hypoxic status but not glucose transport ability in gastric cancer. J Exp Clin Cancer Res. 2013;32(1):34.

Publisher's note